Science of the Total Environment 658 (2019) 424–438

Contents lists available at ScienceDirect

Science of the Total Environment

journal homepage: www.elsevier.com/locate/scitotenv

Combining monitoring and modelling approaches for BaP characterization over a petrochemical area

Noelia Domínguez-Morueco [a,b], Nuno Ratola [c], Jordi Sierra [b,d], Martí Nadal [a], Pedro Jiménez-Guerrero [e,f,*]

[a] Laboratory of Toxicology and Environmental Health, School of Medicine, IISPV, Universitat Rovira i Virgili, Sant Llorenç 21, 43201 Reus, Catalonia, Spain
[b] Environmental Engineering Laboratory, Departament d'Enginyeria Química, Universitat Rovira i Virgili, Av. Països Catalans 26, 43007 Tarragona, Catalonia, Spain
[c] LEPABE-Laboratory for Process Engineering, Environment, Biotechnology and Energy, Faculty of Engineering, University of Porto, Rua Dr. Roberto Frias, 4200-465 Porto, Portugal
[d] Laboratory of Soil Science, Faculty of Pharmacy, Universitat de Barcelona, Avda Joan XXIII s/n, 08028, Barcelona, Catalonia, Spain
[e] Physics of the Earth, Regional Campus of International Excellence "Campus Mare Nostrum", Campus de Espinardo, University of Murcia, 30100 Murcia, Spain
[f] Biomedical Research Institute of Murcia (IMIB-Arrixaca), 30120 Murcia, Spain

HIGHLIGHTS

- BaP in a petrochemical area is characterized using modelling and field-based data
- Atmospheric-soil distribution are obtained for present and future (RCP8.5) climate
- Future atmospheric increases are caused by reduced precipitation and faster oxidation of SVOCs
- Rising temperature and solar radiation leads to enhanced BaP photodegradation in soils
- BaP life-time risk of lung cancer increases by 5×10^{-8} in the most populated areas

GRAPHICAL ABSTRACT

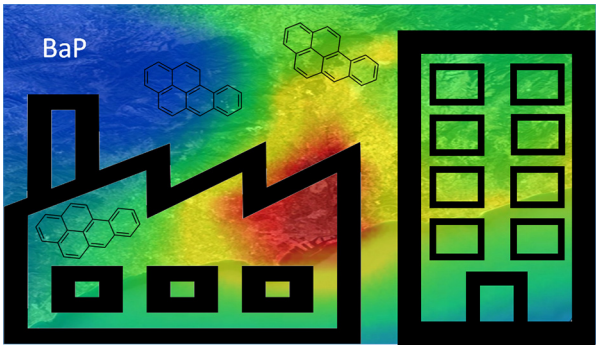

ARTICLE INFO

Article history:
Received 8 May 2018
Received in revised form 13 December 2018
Accepted 13 December 2018
Available online 15 December 2018

Keywords:
Benzo(a)pyrene
Passive sampling
WRF + CHIMERE
Human health
Tarragona (Spain)

ABSTRACT

In this study, air concentrations of BaP in two different seasons (winter 2015 and summer 2016) and BaP levels in ground vegetation from Tarragona County were used as control simulations performed with the WRF-CHIMERE air quality modelling system, in order to reproduce the incidence of that hazardous chemical in air and soils. The CTM was validated for the present climatology, showing a good ability to represent air and soil concentrations of BaP over the target domain (petrochemical, chemical, urban and background sites), particularly in the winter. Then, the variation of the BaP concentrations in air and soils were simulated for the time series 1996–2015 and for the climate change scenario RCP8.5 (2031–2050). While an increase is projected for the levels in air, particularly in chemical and remote sites where the variation can go up to 10%, in terms of soil deposition the findings are the opposite, with an evident decrease in soil BaP concentrations, particularly for background sites. Finally, a potential health effect of BaP for the local population (lung cancer) was assessed. Although according to the projections the EU threshold for BaP atmospheric incidence (1 ng m^{-3}) will not be reached by 2050, there will be an increase in the life-time risk of lung cancer, particularly in the most populated areas within the simulation domain.

* Corresponding author at: Physics of the Earth, , Regional Campus of International Excellence "Campus Mare Nostrum", Campus de Espinardo, University of Murcia, 30100 Murcia, Spain.
E-mail address: pedro.jimenezguerrero@um.es (P. Jiménez-Guerrero).

https://doi.org/10.1016/j.scitotenv.2018.12.202
0048-9697/

1. Introduction

Field sampling is a crucial tool to determine the occurrence of hazardous compounds in the environment. Among the different monitoring strategies, passive sampling of air (with appropriate uptake materials), soils or vegetation can provide information on the levels of many pollutants at different locations including remote areas, with a low-cost and easy maintenance setup (Zabiegała et al., 2010; Cabrerizo et al., 2012; Estellano et al., 2014; Domínguez-Morueco et al., 2017). Nevertheless, to help the transformation of these valuable datasets onto a complete understanding of spatial, temporal and chemical transport patterns it is essential to combine the field observations with modelling tools (Pistocchi et al., 2010; Ratola and Jiménez-Guerrero, 2016; Schneider et al., 2017).

Currently, the mass balance models or deterministic approaches are one of the most used techniques for the modelling of environmental pollutants such as semi-volatile organic compounds (SVOCs), a large group of compounds found worldwide in numerous environmental matrices (He and Balasubramanian, 2010). Mass balance techniques can provide a first approximation of the chemical fate and transport of SVOCs in environmental systems with the fugacity concept, which simplifies the model development and calculations, being used extensively among the scientific community (Mackay and Paterson, 1991; Csiszar et al., 2012, 2013; Domínguez-Morueco et al., 2016). Nevertheless, these techniques do not reflect the complexity of characterising adequately all processes involving these chemicals. In this sense, chemistry transport models (CTMs) such as CHIMERE coupled with the Weather Research and Forecasting (WRF) (the setup used in this work), can complement the field data also considering the meteorology of the study area, the atmospheric chemistry and climate change, contributing to diminish the gaps still existing regarding the environmental behaviour of SVOCs (San José et al., 2013; Ratola and Jiménez-Guerrero, 2015, 2017; Di Guardo et al., 2018). WRF is a numerical weather prediction (NWP) and atmospheric simulation system designed for the understanding and prediction of mesoscale weather (Skamarock et al., 2008), whereas CHIMERE is an Eulerian off-line CTM that includes parameterisations to simulate pollutant concentrations, but still being computationally efficient for forecast applications (Menut et al., 2013).

Table 1
Parameterisations used in the WRF + CHIMERE modelling system.

WRF	CHIMERE
Microphysics → **WSM3**	Chemical mechanisms → **MELCHIOR2**
PBL → **Yonsei University**	Aerosol chemistry → inorganic (thermodynamic equilibrium with **ISORROPIA**) and organic (**MEGAN SOA** scheme) aerosol chemistry
Radiation → **CAM**	Natural aerosols → **dust**, **re-suspension and inert sea-salt**
Soil → **Noah LSM**	Boundary conditions → **LMDz-INCA** + **GOCART**
Cumulus → **Kain-Fritsch**	**EMEP** anthropogenic emissions

Among the different SVOCs, polycyclic aromatic hydrocarbons (PAHs) have attracted the attention of environmental chemists and modellers due to their ubiquity in the environment, constant production/emission, long-range atmospheric transport (LRAT) capacity and relatively high toxicity (Lammel et al., 2009; Estellano et al., 2012; Domínguez-Morueco et al., 2017). For instance, benzo(*a*)pyrene (BaP) has already been classified as carcinogenic to humans (Group 1) by the International Agency for Research on Cancer (IARC), and is the only PAH with a legislated average limit in the atmosphere: 1 ng m^{-3} of BaP over 1 year (European Commission, 2009). International studies suggest that the toxicity and environmental fate and transport of PAHs can be affected by the variations in the temperature and solar radiation associated with climate change, mainly in the most vulnerable regions, such as the Mediterranean basin (Bernalte et al., 2012; Nadal et al., 2015; Marquès et al., 2016a).

PAHs are mostly emitted by anthropogenic sources, being the oil refineries a considerable emission point (Nadal et al., 2009; Odabasi et al.,

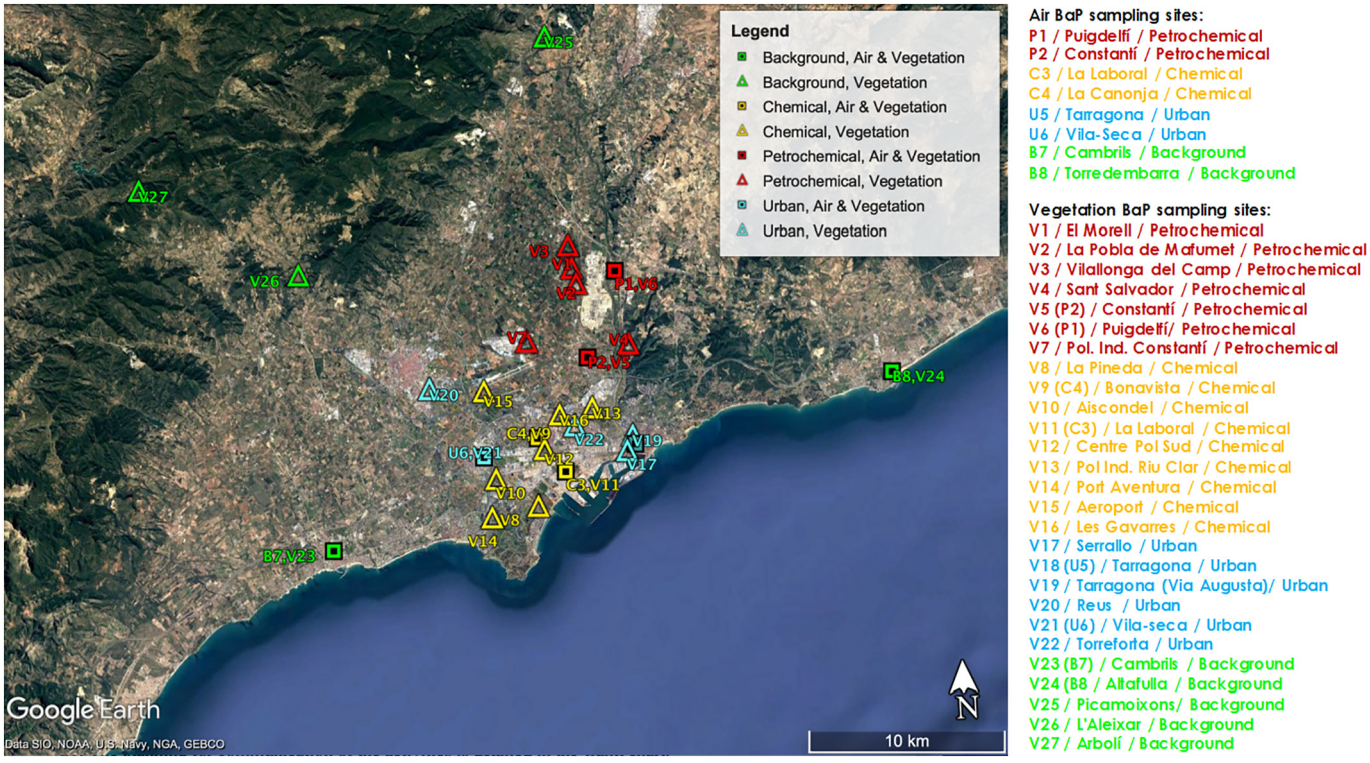

Fig. 1. – Location of sampling sites within the simulation domain (Tarragona). Squares: air+vegetation sampling sites. Triangles: vegetation sampling sites. The colour stands for the characteristics of the site: petrochemical (red), chemical (yellow), urban (blue) and background (green).

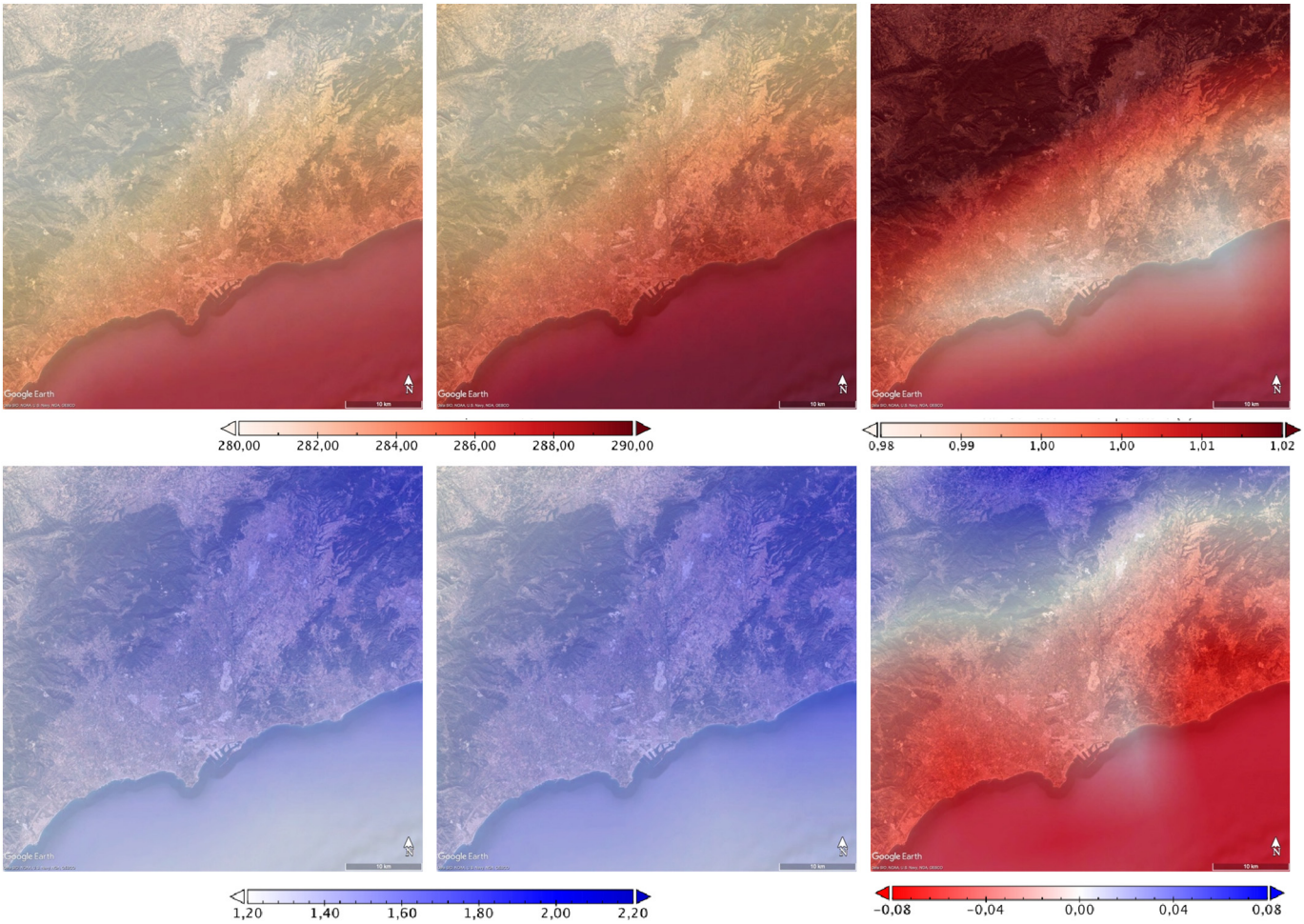

Fig. 2. – Mean near-surface air temperature (top), in K, and precipitation rate (bottom), in mm day^{-1}, for 1996–2015 (left), 2031–2050 (center) and differences between present and future climate conditions under the RCP8.5 scenario (right).

2017). Located in the Mediterranean basin, Tarragona County (Catalonia, NE of Spain) is home to one of the largest chemical/petrochemical complexes in Southern Europe. For this reason, combining monitoring and modelling approaches for PAHs is very important to evaluate the impact of these contaminants in the surrounding environment and to assess the risks for the local population. Thus, associating the results provided by CTMs with the quantitative risk assessment (QRA) methods developed by the European Union can help to unravel potential hazardous effects to human health.

The main aim of this study was to combine monitoring data on air and ground vegetation from Tarragona County with the air quality model WRF + CHIMERE in order to estimate the levels and geographical distribution of BaP in air and soils in a time series between 1996 and 2015 and under the more extreme climate change scenario RCP 8.5 (2031–2050). To achieve this goal the modelling methodology

Table 2
Summary of the comparison of BaP concentrations in air obtained by the chemistry transport model simulations and those estimated from field data, for all stations.

All stations	Winter	Summer
Spatial corr. coef.	0.76	0.71
MFB (%)	1.2	42.1
MAE (pg m^{-3})	6.4	7.2
BIAS (pg m^{-3})	−1.9	2.3
Mean observations (pg m^{-3})	19.8	14.1
Mean CTM (pg m^{-3})	18.0	16.4
STD observations (pg m^{-3})	12.2	11.7
STD CTM (pg m^{-3})	7.9	6.7

CTM – chemistry transport model concentrations; CORR. COEF. – correlation coefficient; STD – standard deviation; MFB - mean fractional bias; MAE – mean absolute error. WINTER (26/11/2014–26/01/2015). SUMMER (01/05/2016–01/07/2016).

Table 3
Results from the comparison of air BaP concentrations in air obtained by the chemistry transport model simulations and those estimated from each individual station.

Code/name/type of station	Mean OBS (pg m^{-3})	Mean CTM (pg m^{-3})	BIAS (pg m^{-3})	MFE (%)
Winter (26/11/2014–26/01/2015)				
P1/Puigdelfí/Petrochemical	40.6	32.5	−8.1	22.2
P2/Constantí/Petrochemical	11.9	20.2	8.3	51.9
C3/La Laboral/Chemical	23.8	18.4	−5.4	25.4
C4/La Canonja/Chemical	21.7	18.4	−3.3	16.5
U5/Tarragona/Urban	16.4	22.5	6.1	31.2
U6/Vila-Seca/Urban	31.6	15.7	−15.8	67.1
B7/Cambrils/Background	4.1	7.9	3.8	63.4
B8/Torredembarra/Background	8.6	8.1	−0.5	5.7
Summer (01/05/2016–01/07/2016)				
P1/Puigdelfí/Petrochemical	32.0	23.2	−8.7	31.6
P2/Constantí/Petrochemical	8.8	18.9	10.1	73.0
C3/La Laboral/Chemical	30.3	19.7	−10.6	42.5
C4/La Canonja/Chemical	17.5	18.1	0.6	3.3
U5/Tarragona/Urban	12.9	23.3	10.4	57.5
U6/Vila-Seca/Urban	4.2	15.0	10.8	113.1
B7/Cambrils/Background	0.9	5.4	4.5	143.1
B8/Torredembarra/Background	6.1	7.5	1.4	21.0

CTM – chemistry transport model concentrations; OBS – observations; MFE - mean fractional error.

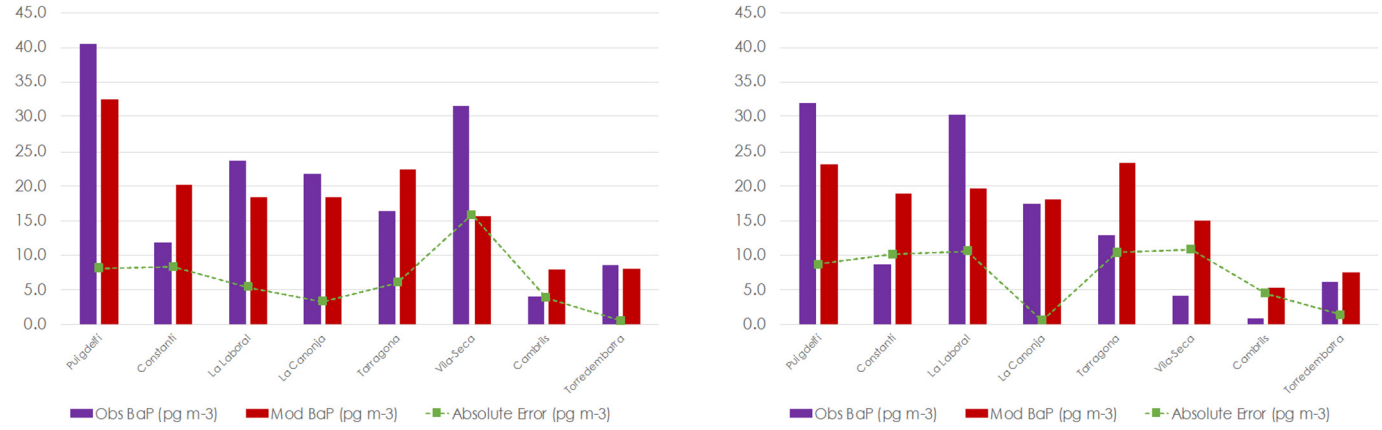

Fig. 3. – (Left) Model evaluation for winter BaP concentrations (pg m^{-3}) (26/11/2014 to 26/01/2015). Violet: observations; Red: CTM concentrations; Green: absolute error. (Right) Id. for summer (01/05/2016 to 01/07/2016).

developed by Ratola and Jiménez-Guerrero (2016) was used. Moreover, in order to assess the potential risk of atmospheric BaP for the local population, a QRA method was conducted, concerning the risk of lung cancer associated to the presence of BaP in the atmosphere of Tarragona County.

2. Materials and methods

2.1. Field sampling

In this study, the BaP concentrations of air and vegetation samples collected for a monitoring study in Tarragona County (reported in Domínguez-Morueco et al., 2018) were used in order to evaluate the WRF + CHIMERE modelling system (Fig. 1). The sampling strategy is explained in brief below:

For air, passive air samplers (PAS) with pre-cleaned polyurethane foams (PUF disks; diameter: 14 cm; thickness: 1.2 cm; surface area: 360 cm^2; density: 0.035 g cm^{-3} from Newterra, Beamsville, ON, Canada) were used to measure the atmospheric BaP levels in Tarragona County. A total of eight PAS were deployed in different areas for a period of 2 months in two different sampling campaigns: from 26/11/2014 to 26/01/2015 and from 01/05/2016 to 01/07/2016. The distribution of the sampling sites was reported previously by Domínguez-Morueco et al., 2017 (two samples in a petrochemical area, P1 and P2; two samples close to a zone of chemical industries, C3 and C4; two samples in urban areas, U5 and U6; and two samples in background sites, B7 and B8, 30 km away from the area of influence of all suspected sources of contamination).

Regarding vegetation, a total of 27 samples were collected by the end of January 2016 (25/01/2016) in different zones of Tarragona County (7 in the petrochemical area; 9 in the chemical area; 6 in residential and urban zones of Tarragona and 5 in background locations). A total of 50 g of vegetation samples (*Piptatherum paradoxum* L.) were obtained by cutting the plants 5 cm above ground, and further drying them at room temperature.

2.2. Analysis and quantification of field samples

The analysis and quantification of BaP in environmental samples was done together with other PAHs, as reported by Domínguez-Morueco et al. (2018).

In brief, and in the case of air samples, BaP was extracted from PUFs using Soxhlet and a clean-up strategy similar to that described by Silva et al. (2015). The Soxhlet method consisted in extracting with 250 mL Hex/DCM (1:1) overnight and reduces the extracts to 1 mL in a rotary evaporator before clean-up, which consisted of two steps. First, SPE glass columns packed with 5 g of alumina, conditionined with 50 mL of DCM:Hex (1:1) and eluted after sample loading with 50 mL of the same solvent. The extract was then reduced to 1 mL on a rotary evaporator and loaded onto GPC glass columns containing 6 g of S-X3 Biobeads for the second step. Elution was done with 40 mL of DCM: Hex (1:1), from which the first 15 mL were rejected and the remaining eluate collected. The extract volume was again reduced to about 1 mL in rotavapor, followed by evaporation to dryness under a gentle stream of nitrogen. Sample reconstitution was done with 100 μL of hexane before analysis by GC–MS. For vegetation samples, BaP was extracted by ultrasound extraction method followed by a QuEChERS clean-up step (work submitted for publication). A total of 2.5 g of vegetation were transferred into 50 mL Falcon tubes and extracted with 20 mL Hex:DCM (2:1) in a sonication bath for 10 min. Then, the content of the QuEChERS 1 (6 g of $MgSO_4$ and 1.5 g of CH_3COONa) was added to each Falcon tube and vortexed for 3 min. Subsequently, the tubes were centrifuged for 10 min and the supernatant collected and transferred to the QuEChERS 2 (0.9 g of $MgSO_4$, 0.15 g of alumina, 0.15 g Florisil and 0.15 g of C_{18}). The tubes were shaken again during 3 min in order to conduct the dispersive solid-phase extraction (d-SPE), centrifuged for 10 min and the extract collected and filtered with a conventional 0.2 μm size filter in order to enhance the clean-up. The final sample extract was concentrated until dryness with nitrogen and re-dissolved with 100 μL of hexane before the GC–MS analysis. The details of the chromatographic analysis can be found in Silva et al. (2015).

2.3. Set-up and validation of the modelling approach

The modelling methodology chosen follows the work developed by Ratola and Jiménez-Guerrero (2016). In this case, the WRF + CHIMERE modelling system with a resolution of 2 km for the Catalonia (Spain) domain was used. A nesting approach was followed, with three two-ways nesting domains covering the Iberian Peninsula (18 km horizontal resolution), the Spanish Levantine Coast (6 km) and Catalonia (2 km). For present-day reanalysis simulations (1996–2015), lateral boundary conditions were provided every 6 h from the ERA-Interim reanalysis of the European Center for Medium-Range Weather Forecast (ECMWF; Dee et al., 2011). WRF + CHIMERE was coupled to the BaP emissions given by the European Monitoring and Evaluation Programme (EMEP; Vestreng et al., 2009). The EMEP dataset is compiled from BaP emissions officially reported by the parties under the convention on Long-Range Transport, which can lead to large differences in data quality for different countries (Bieser et al., 2012). San José et al. (2013) estimate that the uncertainty in the emission inventories regarding PAHs are estimated to be within a factor of 2 to 5. Particularly, it should be highlighted that the EMEP emission database has significant gaps in the spatial coverage in reporting of emission data for individual persistent organic pollutants (POPs) or related groups of chemicals

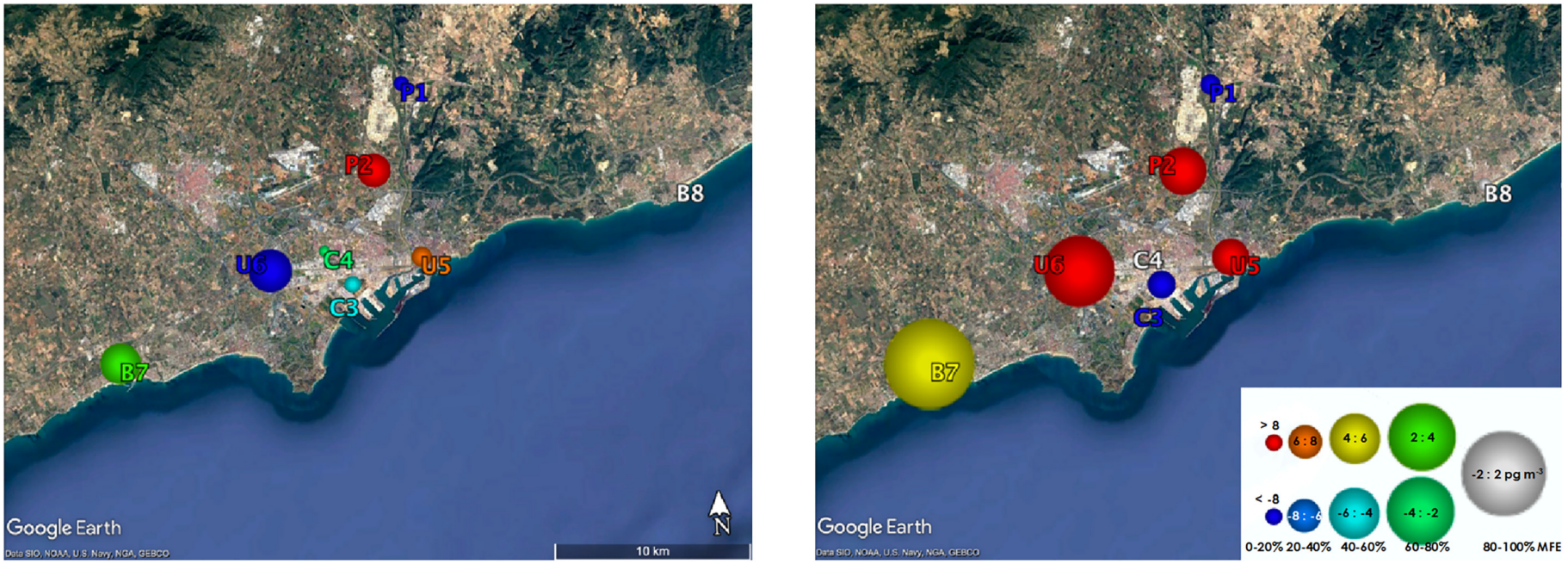

Fig. 4. – Biases and mean fractional error (MFE) for winter (left) at each air sampling site for BaP concentrations (26/11/2014 to 26/01/2015). The colour represents the bias (pg m^{-3}), while the size stands for the MFE (%). (Right) Id. for summer (01/05/2016 to 01/07/2016).

Table 4
Summary of the results from the comparison of airborne BaP deposition in soil by the chemistry transport model simulations and those estimated from the levels in *P. paradoxum* collected on 25/01/2016, for all sampling points ($n = 27$).

All sampling points	
Spatialcorr. coef. (R)	0.83
MFB (%)	−7.90
MAE (ng g^{-1})	0.12
BIAS (ng g^{-1})	−0.03
Mean observations (ng g^{-1})	0.50
Mean CTM (ng g^{-1})	0.47
STD observations (ng g^{-1})	0.47
STD CTM (ng g^{-1})	0.43

CTM – chemistry transport model; CORR. COEF. – correlation coefficient; STD – standard deviation; MFB - mean fractional bias; MAE – mean absolute error.

(Breivik et al., 2006). The CHIMERE version was modified to include BaP in gaseous and particulate phase after Ratola and Jiménez-Guerrero (2015, 2016, 2017). The main parameterisations are presented in Table 1.

The lighter PAHs (2 or 3 aromatic rings) exist mainly in the gas phase, whereas the heavier ones (5 to 6 rings) consist almost entirely of particulate phase (Srogi, 2007), which is the case of 5-ringed BaP modelled in this work. Thus, BaP is introduced in the model as three different types at the same time: primary, semivolatile and reactive. First-order gas-phase degradation by OH radicals, which represents over 99% of the degradation path for gas-phase BaP, was accounted for, with a $k_{OH} = 5.68 \times 10^{-11}$ cm^3 $molecule^{-1}$ s^{-1} (Schwarzenbach et al., 2003). The oxidation of particulate BaP with O_3 was also included, since the respective reaction rate is one order of magnitude higher than other degradation processes, and can be considered the only effective degradation path for particulate BaP in the atmosphere (Bieser et al., 2012). In this case, the reaction constant follows the approach of Pöschl et al. (2001):

$$k = k_{max}\,[O_3]\,(1 + K_{O3}\,[O_3]) \quad (1)$$

being $k_{max} = 0.015$ s^{-1} and $K_{O3} = 2.8 \times 10^{-13}$ cm^3.

The model system was run and evaluated for a simulation covering a time frame coinciding with the passive air samples. That is, for a winter (26/11/2014 to 26/01/2015) and a summer (01/05/2016 to 01/07/2016) period, in order to check the ability of the model to reproduce BaP climatologies over the target area. Moreover, the deposition in soils is assessed against the concentrations of BaP found on *Piptatherum paradoxum* L. samples collected on 25/01/2016. *P. paradoxum* is a fast-growing grass (life cycle between 2 and 4 months), beginning its growth with the first rains and when temperatures begin to drop, and drying up during the warm seasons (Sulas et al., 2015). Moreover, being a ground plant with low height, the concentration accumulated during its lifetime can be a good representation of the deposition onto the soil. Therefore, the deposition period extracted from the model is considered to be three months, in line with the plant's lifetime.

To assess the ability of the model to reproduce current BaP air concentrations, a number of statistical parameters were tested for atmospheric levels and soil deposition. For instance, spatial correlation coefficient (R), mean absolute error (MAE) and mean bias (Bias) are commonly used by modellers. In addition, according to Boylan and Russell (2006), the mean fractional bias (MFB) and the mean fractional error (MFE) were also used. These authors indicate that the model performance criterion is met when MFE ≤ 75% and MFB ≤ ±60%. As such, these criteria were chosen to supply the metrics for the evaluation of BaP by the WRF + CHIMERE modelling system.

After the ability of the model is analysed, its accuracy for reproducing the BaP climatologies correctly was assessed, with present and future simulations run with WRF + CHIMERE modelling system. The air quality associated to the BaP levels in this work uses simulations spanning the reference period 1996–2015 for the present, and 2031–2050 under the RCP8.5 scenario (Moss et al., 2010), as a future-enhanced forcing scenario. This RCP8.5 scenario was chosen because it provides an upper estimate of the projected climate forcing (Meinshausen et al., 2011; Taylor et al., 2012), maximizing the impact of the change in CO_2 concentration (Yu et al., 2014) and hence provoking its warming signal to exceed significantly the natural interannual variability (Lang et al., 2015).

To date, the future-minus-present method has been the most frequent approach adopted for the evaluation of climate change impacts on projected regional air quality. This is based on the assumption that biases in simulated present-day and future climate simulations should tend to cancel each other, and thus their difference captures the signal of the concentration anomalies. This method is widely supported in most future climate-air quality interactions studies (e.g. Liao et al., 2009; Jiménez-Guerrero et al., 2013a, 2013b, 2013c), and therefore followed in this work. Simulations for present-day climatologies (1996–2015) were compared to a time slice covering 2031 to 2050. For these simulations, the modelling methodology is analogous as described above for the reanalysis, but lateral boundary conditions and forcing were taken from the CMIP5-experiment r1i1p1 MPI-ESM-LR historical and RCP8.5 run (Giorgetta et al., 2012a, 2012b). In order to isolate the possible effects of climate change on the ground concentrations of air pollution, unchanged anthropogenic emissions are assumed. Natural emissions depend on climate conditions and, consequently, are the only ones to vary between reference and future climate simulations. Thus, the effects of climate change on air pollutants are estimated without considering possible changes on vegetation, land use, anthropogenic pollutant emission changes or any feedbacks from the chemical compounds to the meteorological fields, but allowing changes in natural emissions (e.g. Meleux et al., 2007; Jiménez-Guerrero et al., 2012). Biogenic emissions were generated dynamically using MEGAN (Model of Emissions of Gases and Aerosols from Nature) with the parameterised form of the canopy environment model (Guenther et al., 2006). The model estimates these emissions as a function of hourly temperature and ground level shortwave radiation from WRF.

The differences between these two time slices will provide the changes in future BaP levels referring both to atmospheric concentrations and soil levels. The WRF + CHIMERE model ability to reproduce present and future climatologies over the Iberian Peninsula has been assessed in a number of previous works (e.g. Jiménez-Guerrero et al., 2012, 2013a, 2013b, 2013c; Jerez et al., 2013a, 2013b). The projections over the Tarragona area (Fig. 2) indicate an increase in temperature around 1.0 K (practically constant over the target area), while precipitation decreases (increases) 5×10^{-7} kg m^{-2} s^{-1} (0.04 mm day^{-1}) in the southern (northern) part of the domain.

3. Results and discussion

This section presents the results of the evaluation of the model against observed BaP concentrations: atmospheric levels (Section 3.1) and soil deposition (Section 3.2). Section 3.3 presents the present (1996–2015) and future (2031–2050, RCP8.5 scenario) climatologies of BaP, while Section 3.4 discuss possible impacts on human health for current and future BaP atmospheric levels.

3.1. Evaluation of atmospheric BaP levels

The simulated BaP concentrations are here assessed for a winter and a summer period (26/11/2014 to 26/01/2015 and 01/05/2016 to 01/07/2016, respectively, corresponding to the timeframe of the passive sampling campaigns). When model simulations are evaluated against the passive air samplers (PUFs) observations, all the statistical parameters estimated (see Table 2) indicate that the model tends to perform better for winter than for summer, (e.g., the mean

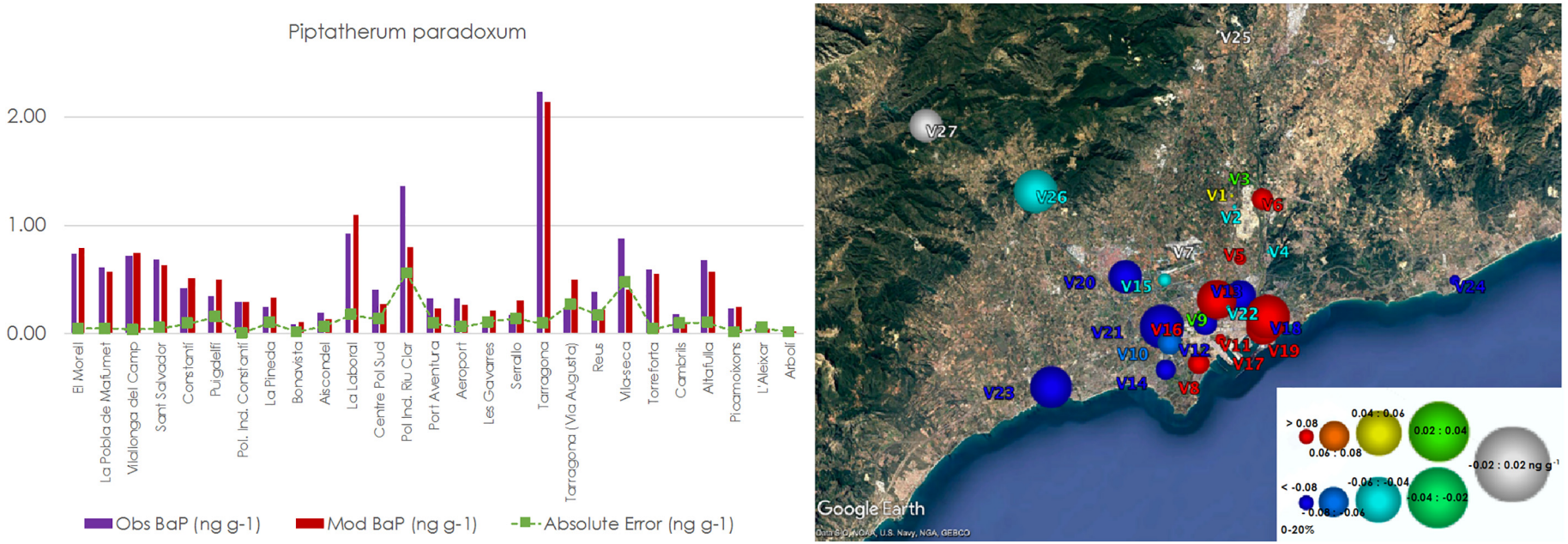

Fig. 5. – (Left) Model evaluation for 3-month soil deposition of BaP (ng g^{-1}) against *P. paradoxum* concentrations (collected on 25/01/2016). Violet: observations; Red: CTM concentrations; green: absolute error. (Right) Id. for biases and mean fractional error (MFE). The colour represents the bias (pg m^{-3}), while the size stands for the MFE (%).

Table 5
Comparison of BaP deposition in soil by the CTM simulations and those estimated from the levels in *P. paradoxum* collected on 25/01/2016, for each individual station.

Code	Name	Type of station	Mean OBS (ng g^{-1})	Mean CTM (ng g^{-1})	BIAS (ng g^{-1})	MFE (%)
V1	El Morell	Petrochemical	0.74	0.79	0.05	6.21
V2	La Pobla de Mafumet	Petrochemical	0.61	0.57	−0.04	7.41
V3	Vilallonga del Camp	Petrochemical	0.71	0.75	0.03	4.68
V4	Sant Salvador	Petrochemical	0.68	0.63	−0.05	7.99
V5 (P2)	Constantí	Petrochemical	0.42	0.51	0.09	19.24
V6 (P1)	Puigdelfí	Petrochemical	0.35	0.50	0.16	36.61
V7	Pol. Ind. Constantí	Petrochemical	0.29	0.30	0.01	2.21
V8	La Pineda	Chemical	0.24	0.34	0.10	35.23
V9 (C4)	Bonavista	Chemical	0.09	0.11	0.02	15.68
V10	Aiscondel	Chemical	0.19	0.13	−0.07	40.55
V11 (C3)	La Laboral	Chemical	0.92	1.09	0.18	17.50
V12	Centre Pol Sud	Chemical	0.41	0.28	−0.13	38.76
V13	Pol Ind. Riu Clar	Chemical	1.37	0.80	−0.56	51.86
V14	Port Aventura	Chemical	0.33	0.24	−0.09	32.80
V15	Aeroport	Chemical	0.33	0.27	−0.06	21.25
V16	Les Gavarres	Chemical	0.11	0.22	0.11	65.55
V17	Serrallo	Urban	0.17	0.31	0.14	57.70
V18 (U5)	Tarragona	Urban	2.23	2.14	−0.09	4.12
V19	Tarragona (Via Augusta)	Urban	0.23	0.50	0.27	74.64
V20	Reus	Urban	0.39	0.22	−0.17	55.71
V21 (U6)	Vila-seca	Urban	0.88	0.41	−0.48	74.12
V22	Torreforta	Urban	0.60	0.56	−0.04	7.04
V23 (B7)	Cambrils	Background	0.18	0.09	−0.09	69.07
V24 (B8)	Altafulla	Background	0.67	0.57	−0.10	16.07
V25	Picamoixons	Background	0.23	0.24	0.01	5.29
V26	L'Aleixar	Background	0.09	0.04	−0.05	72.47
V27	Arbolí	Background	0.03	0.02	−0.01	54.78

CTM – chemistry transport model concentrations; OBS – observations; MFE - mean fractional error.

fractional bias, MFB, is 1.2% and 42.1%, respectively). In general, the spatial correlation coefficient (R) indicates an accurate representation of BaP spatial patterns over the target area (R from 0.71 in summer to 0.76 in the winter, respectively). Still, the representation of the variability of the atmospheric concentrations is underestimated by the CTM in both seasons, with underpredictions around 5 pg m^{-3} of the spatial standard deviation. These are general findings that apply to the whole domain. Further analysis done considering relevant aspects within the area of study (petrochemical areas, chemical, urban or background sites) is presented below.

In fact, regarding the different site types considered (petrochemical, chemical, urban and background), the CTM can generally describe the differences seen in the BaP loads (Table 3). The distribution of the observed concentrations follow a general decreasing trend from petrochemical/chemical areas to urban and to remote sites (min 0.9 pg m^{-3} for the remote site of Cambrils, B7, in summer –with a corresponding modelled value of 5.4 pg m^{-3}- and max of 40.6 pg m^{-3} for the Puigdelfí petrochemical site, P1, in winter, with modelled concentrations of 32.5 pg m^{-3}) (Fig. 3). In this case, the typical seasonal trend observed for PAHs in the atmosphere is verified, with higher atmospheric loads of BaP in winter and lowest in summer (Srogi, 2007). This is observed in all stations except in La Laboral (C3; 23.8 vs. 30.3 pg m^{-3} in winter and summer, respectively). This station (La Laboral) is the closest station to the Tarragona port, and therefore the seasonality of the emissions (associated to cruises and other vessels, with a higher activity during summer months) can condition the summer and winter BaP levels.

The modelling results observed for the mean CTM concentrations indicate a different seasonal pattern, with lower biases and MFBs (meaning more accurate results) in winter than in summer (Fig. 4). Summer levels are, in general, overpredicted by the model, while winter concentrations are slightly underestimated. The highest errors are found in the background station of Cambrils (B7), where both wintertime and summertime BaP concentrations are overpredicted (MFB of 63.4% and 143.1%, respectively), due to an overestimation in the background values of BaP prescribed as initial and boundary conditions in the simulations. However, the low levels at this station tend to increase the percent bias, while the absolute bias is just under 5 pg m^{-3} in both seasons. On the other hand, the lowest biases are found at La Canonja (C4) chemical site (MFB of 3.3% and −16.5% in summer and winter, in that order). In general, the model presents the most accurate results over the chemical/petrochemical sites. The MFEs for each individual site are below 75% for the majority of the site types and corresponding seasons (except for U6 and B7 in summertime), complying with the model performance criterion of MFE ≤ +75% (Boylan and Russell, 2006). These results help building confidence for the use of the CTM as a good representation for atmospheric levels of BaP, and therefore as a useful tool to assess the variations of BaP in present climate scenarios.

3.2. BaP levels of soil deposition

The modelled soil deposition was compared to data from BaP levels obtained in the ground plant *P. paradoxum* collected in field sampling campaigns in the Tarragona domain (Domínguez-Morueco et al., 2018). A 3-month deposition period was selected, since it is considered to be coincident with the lifetime of this biomonitor. Table 4 summarises the main statistical validation parameters considered for all 27 sampling sites (8 of them coinciding with those of the passive air samples).

Results show a good agreement between the field monitoring and the modelling approach, which has in general an overall good capacity to describe the deposition of BaP. The spatial coefficient of correlation (R) is even higher than for atmospheric concentrations (0.83), indicating a good performance of the model to reproduce the spatial variability of the sampling sites. Simulations tend to slightly underestimate the sampled concentrations (MFB −7.9%, BIAS −0.03 ng g^{-1}) and the standard variation (0.47 ng g^{-1} in observations and 0.43 ng g^{-1} in the model).

There are, however, some facts worth to mention regarding the behaviour for each site (Fig. 5 and Table 5). In petrochemical areas, the model is likely to produce very accurate results, with errors generally under 10% (average MFE of 12.05%, and ranging from 6.21% (El Morell) to 36.61% (Puigdelfí, P1 site). On the other hand, background

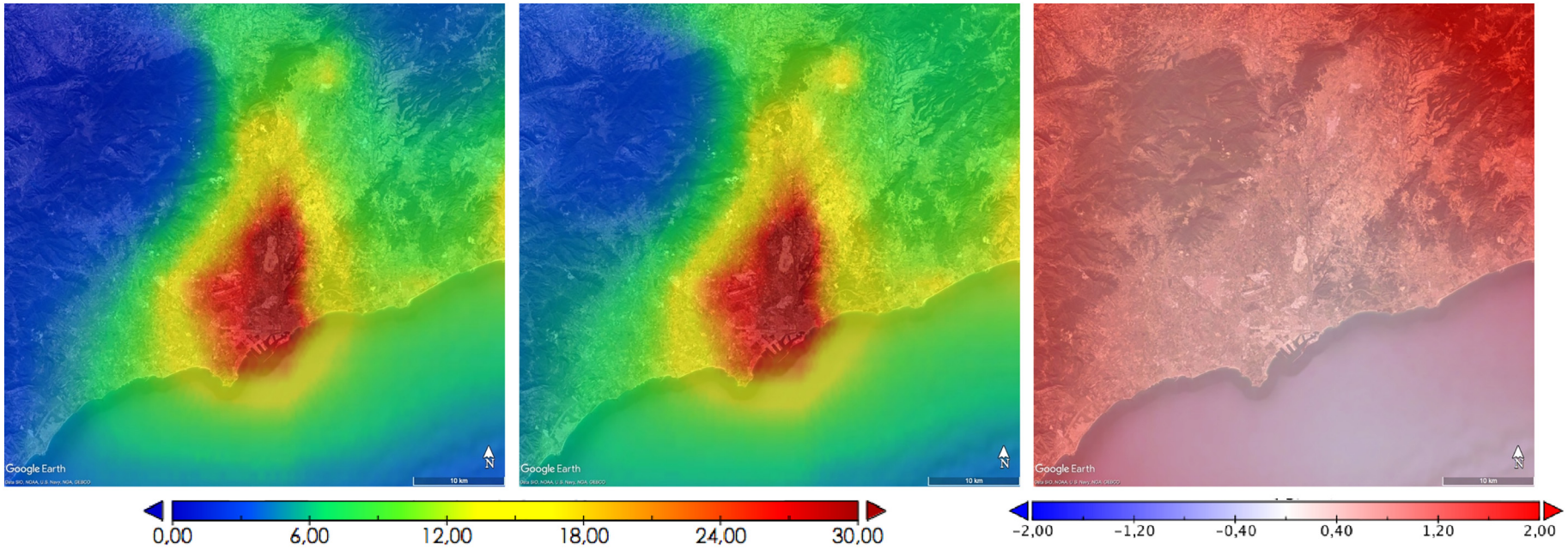

Fig. 6. – BaP atmospheric concentration (pg m^{-3}) for the time periods 1996–2015 (left) and 2031–2050 (center), and differences between present and future climate conditions under the RCP8.5 scenario (right).

Table 6
Comparison of present (1996–2015) and future (2031–2050) atmospheric BaP concentrations given by the CTM simulations.

Code/name/type of station	Present (pg m^{-3})	Future (pg m^{-3})	ΔBaP (pg m^{-3})	ΔBaP (%)
P1/Puigdelfí/Petrochemical	26.0	27.0	0.9	3.6
P2/Constantí/Petrochemical	19.5	20.4	0.9	4.8
C3/La Laboral/Chemical	18.7	19.8	1.1	6.0
C4/La Canonja/Chemical	18.2	19.9	1.7	9.1
U5/Tarragona/Urban	22.8	22.8	0.0	0.1
U6/Vila-Seca/Urban	15.4	15.5	0.1	0.5
B7/Cambrils/Background	5.2	5.7	0.5	10.0
B8/Torredembarra/Background	7.7	8.2	0.5	6.4

and urban areas are generally underestimated by the model, exhibiting the largest errors (MFEs of 43.45% and 45.55%, respectively). The maximum MFE is 74.64% in the urban sampling site of Tarragona-Vía Augusta. The mean MFE in chemical sites is 35.46% (ranging from 15.68% in Bonavista, C4, to 65.55% in Les Gavarres). Petrochemical chemical and urban areas have a strong influence from local emissions, but the higher error found for urban stations may point towards a worse representation in BaP emissions from traffic than for industrial activities in the emission inventory.

In light of these findings, the evaluation indicates that the model presents a good ability to represent BaP atmospheric levels and soil deposition in Tarragona, especially for areas related to petrochemical and chemical industries, which are often hot spots of contamination.

3.3. BaP climatologies and future climate scenario

3.3.1. Climatologies of atmospheric BaP concentrations

Since most of the BaP concentrations reported by the model are in the particulate phase, the response of this component to changes in future climate conditions varies as previously reported for aerosols in the Iberian Peninsula (Jiménez-Guerrero et al., 2012). As a first guess, the higher temperatures modelled by WRF + CHIMERE in the target domain (Fig. 2) favour SVOCs to remain in the gas phase. Moreover, low molecular weight PAHs are more rapidly volatilized from soils with increased temperatures, as will be discussed in Section 3.3.2. On the other hand, the modelled increases in temperatures and specific humidity may also result in a faster oxidation of SVOCs, increasing the formation of condensable compounds (Liao et al., 2009). The slight increase in BaP concentrations (in the order of 0.5 pg m^{-3}, Fig. 6) may suggest that chemical production effects are outweighing volatility effects, as also stated by Dawson et al. (2009). Moreover, precipitation drives the change in the concentration of aerosols. The slight decrease in precipitation projected for the southern part of the target domain in the RCP8.5 scenario with respect to current levels (around 3%) leads to a regional increase in the BaP concentrations in 2031–2050. The rise in condensable compounds is also facilitated by the decrease of precipitation, the main sink for these chemicals (Jiménez-Guerrero et al., 2012).

An important remark has to be done regarding the inherent uncertainties in the climate projections which may affect the results depicted here. Not all climatic variables are affected by the same degree of uncertainty. Future climate simulations tend to agree in a warm trend due to the increase of greenhouse gases concentrations, only differing in the intensity and spatial distribution details. However, there is not such a good agreement in the projections of precipitation changes, which strongly affect the results for BaP. This larger uncertainty is partly due to the complex mechanism that governs precipitation, which involves a wide variety of spatial scales and it is approximated by different approaches among the state-of-the-art models.

Table 6 compares the modelled present and future BaP concentrations for each of the passive air sampling stations. It can be seen that in all cases an increase in those levels is projected, but interestingly with less extent in the urban areas. In fact, the variation is almost none, which may be an indication that the emissions of particulate matter could cancel the effect of the temperature rise and the consequent volatilisation affect. On the other hand, chemical and remote sites will suffer the strongest variations, up to 10% in Cambrils (B7). The aforementioned decrease in precipitation could be responsible for a lower wet deposition of the particulate material, hence increasing the atmospheric loads, but also it is expected that with the rise in population, the background sites will have more urban pressure and thus more emission sources.

3.3.2. Climatologies of BaP concentrations for soil deposition

Climate change induces variations in some environmental factors, such as temperature, precipitation (Fig. 2) or UV-B radiation. These factors alter the fate and behaviour of a wide range of chemicals, due their influence over natural processes such as the environmental partitioning or chemical transformation (Noyes et al., 2009; EL-Saeid et al., 2015; Jia et al., 2015). In our case, future soil concentration (estimated as the average of the accumulated 3-month deposition over ground vegetation; Fig. 7) decreases up to 1.0 ng g^{-1} in the RCP8.5 scenario when 1996–2015 vs. 2031–2050 concentrations are compared. A number of studies focusing on PAHs have identified photodegradation as an important transformation pathway (Zhang et al., 2006). Our results point out that increasing the temperature and the solar radiation (as derived from the climate change projections shown in Fig. 2) lead to an increase in the photodegradation of BaP. This agrees with a number of laboratory studies and others performed under field conditions (Marquès et al., 2016b, 2017), indicating that low molecular weight PAHs are more rapidly volatilized from soils while medium and high molecular weight PAHs showed higher photodegradation rates.

Some PAH metabolites can be generated as photodegradation by-products, such as a variety of aldehydes, oxy-, hydroxy- and nitro-PAHs (Marquès et al., 2017) that could be even more toxic than their parental compounds (Huang et al., 1995; Mallakin et al., 1999; Ras et al., 2009). Recently, international studies have evaluated the influence of climate change over PAH photodegradation in Mediterranean soils (Marquès et al., 2016a, 2016b, 2017) and showed that, apart from the molecular weight of each hydrocarbon, the photodegradation of PAHs in soils is highly dependent on the exposure time, the soil texture (especially in soils with a finer fraction), and on the presence of semiconductor minerals, such as metal oxides (Marquès et al., 2016a). This means that a reduction in the BaP soil deposition is not necessarily a reduction in the overall hazardous effects, if attributed to its metabolites.

Table 7 compares the present and future BaP levels for each sampling site. The projected decrease is clear and follows an inverse pattern to the levels in air. In fact, the decreases of BaP in the soils are higher (lower) for those sites where in the atmosphere the increase was lower (higher), namely the urban (background) sites, in this case. This trend is not surprising, since a rise in the levels in atmospheric BaP can also indicate that the deposition processes are not so effective. Emissions obviously play a very important part in this equation and it is clear that in this domain there are numerous local sources that are contributing to the BaP distribution and behaviour and that need to be continuously monitored, combining field sampling strategies and modelling approaches.

3.4. Assessment of increased health risks associated to atmospheric BaP

The benefits of the use of CTMs to describe the presence and behaviour of priority pollutants can be remarkable, even regarding human health issues. Thus, it is also the intention of this study to provide an example of how these tools can help in the assessment (and correction) of

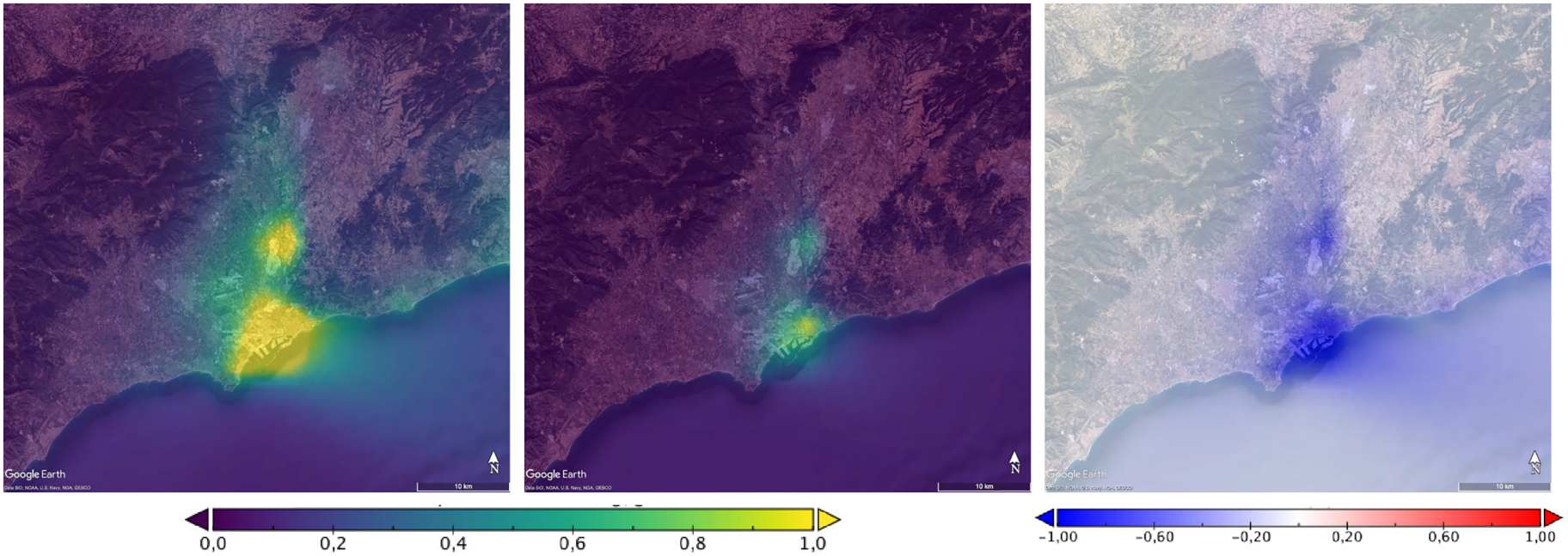

Fig. 7. – BaP mean concentration in soils (ng g^{-1}) for 1996–2015 (left), 2031–2050 (center) and differences between present and future climate conditions under the RCP8.5 scenario (right).

Table 7
Comparison of present (1996–2015) and future (2031–2050) BaP concentration in soil given by the CTM simulations.

Code	Name	Type of station	Present ($ng\ g^{-1}$)	Future ($ng\ g^{-1}$)	ΔBaP ($ng\ g^{-1}$)	ΔBaP (%)
1	El Morell	Petrochemical	0.89	0.59	−0.30	−33.88
2	La Pobla de Mafumet	Petrochemical	0.75	0.53	−0.22	−29.43
3	Vilallonga del Camp	Petrochemical	0.89	0.59	−0.30	−33.88
4	Sant Salvador	Petrochemical	0.50	0.37	−0.13	−25.57
5 (P2)	Constantí	Petrochemical	1.02	0.78	−0.24	−23.53
6 (P1)	Puigdelfí	Petrochemical	1.39	1.17	−0.22	−15.51
7	Pol. Ind. Constantí	Petrochemical	0.59	0.35	−0.24	−40.30
8	La Pineda	Chemical	1.09	0.68	−0.41	−37.33
9 (C4)	Bonavista	Chemical	1.29	1.12	−0.18	−13.61
10	Aiscondel	Chemical	0.43	0.22	−0.22	−49.99
11 (C3)	La Laboral	Chemical	1.91	1.42	−0.49	−25.68
12	Centre Pol Sud	Chemical	0.77	0.50	−0.27	−34.63
13	Pol Ind. Riu Clar	Chemical	1.02	0.78	−0.24	−23.53
14	Port Aventura	Chemical	0.54	0.26	−0.28	−51.29
15	Aeroport	Chemical	0.58	0.32	−0.25	−43.88
16	Les Gavarres	Chemical	1.29	1.12	−0.18	−13.61
17	Serrallo	Urban	2.06	1.89	−0.17	−8.19
18 (U5)	Tarragona	Urban	2.06	1.91	−0.15	−7.10
19	Tarragona (Via Augusta)	Urban	0.97	0.68	−0.29	−30.27
20	Reus	Urban	0.39	0.17	−0.22	−55.52
21 (U6)	Vila-seca	Urban	0.43	0.22	−0.22	−49.99
22	Torreforta	Urban	1.29	1.12	−0.18	−13.61
23 (B7)	Cambrils	Background	0.19	0.04	−0.15	−80.70
24 (B8)	Altafulla	Background	0.32	0.08	−0.23	−74.21
25	Picamoixons	Background	0.39	0.10	−0.29	−74.66
26	L'Aleixar	Background	0.08	0.01	−0.08	−93.12
27	Arbolí	Background	0.04	0.00	−0.04	−97.88

potentially hazardous effects on humans related to the atmospheric presence of BaP.

When the European Union was trying to set target values for arsenic, cadmium, mercury, nickel and polycyclic aromatic hydrocarbons in ambient air in the Directive 2004/107/EC, a Quantitative Risk Assessment (QRA) method was based on different studies, such as Andersen et al. (1982), Lindstedt and Sollenberg (1982) or RIVM (1989) and laid out in the "Ambient air pollution by Polycyclic Aromatic Hydrocarbons (PAH)" Position Paper (European Union, 2001). These studies focused on the increased risk of lung cancer due to the industrial exposure to PAHs. Using this method and the World Health Organisation unit risk of lung cancer estimate (87×10^{-6} BaP m^{-3} for lifetime exposure) for PAH compounds (World Health Organisation, 2000), the European Union calculated the increased risk for three possible target values: (1) 0.01 ng m^{-3} with an associated increased life-time risk of 1×10^{-6}; (2) 0.1 ng m^{-3} (increased risk of 1×10^{-5}); and (3) 1 ng m^{-3} (increased risk of 1×10^{-4}). Based on the health evidence and acceptance that the upper limit of the additional life-time risk should be $<1 \times 10^{-4}$, the European Union decided on a target value for the annual mean concentration of BaP of 1 ng m^{-3} (Butterfield and Brown, 2012), which is the one set in the Directive 2004/107/EC (European Commission, 2009).

As seen in Fig. 8, and despite being a potential hot spot for atmospheric contamination, our domain stays far from the target values of 1 ng m^{-3} and even of 0.1 ng m^{-3} in both present and future simulations. In fact, while some areas downwind from the petrochemical complex of Tarragona exceed the target value of 0.01 ng m^{-3} (10 pg m^{-3}, with an associated increased life-time risk of 1×10^{-6} for lung cancer), the rest of the Tarragona domain stays below it. Moreover, the changes under RCP8.5 are not noticeable, with only an extension of the area exceeding the 0.01 ng m^{-3} target value, and an increase in the most populated areas of 5×10^{-8} in the life-time risk of lung cancer. This is a direct consequence of the aforementioned low changes modelled for the BaP air levels in the Tarragona domain.

4. Conclusions

This work intended to highlight the current presence of BaP in such a complex domain as the Tarragona petrochemical area and how future climate change can influence its atmospheric levels for the middle 21st century. To that aim, a regional climate modelling system (coupling WRF and CHIMERE chemistry transport model) was used. Simulations, with a final resolution of 2 km (three-domain nested approach) used ERA-Interim and CMIP5-experiment r1i1p1 MPI-ESM-LR historical and RCP8.5 run forcings and lateral boundary conditions. Validation of the model was done using field-based data from passive air sampling and ground vegetation to represent soil deposition and after that, simulations were run for two time slices covering a present-climate condition (1995–2016) and the future RCP8.5 scenario (2031–2050) in order to obtain regional distributions of atmospheric and soil BaP levels. This RCP8.5 scenario was chosen because it provides an upper estimate of the projected climate forcing and temperature response greatly exceeds that of inter-annual variability.

Results show a good performance of the CTM to represent air and soil concentrations of BaP over the Tarragona County (considering petrochemical, chemical, urban and background sites) with better results in the winter. The plausible influence of climate change alone on the levels of gas-phase pollutants and aerosols is also acceptable. The findings of this study indicate that the enhanced oxidative capacity of the atmosphere together with the decrease in precipitation projected for the RCP8.5 scenario causes gas-phase emissions to turn into the particulate phase, thus slightly increasing atmospheric BaP concentrations in future climate change scenarios. On the other hand, photodegradation has a role in the variation (decrease) of future soil deposition and concentration. This photodegradation process can be very important in a region such as the Mediterranean basin, with a strong presence of sunlight during the whole year and also referred as a zone vulnerable to climate change (Marquès et al., 2016b). And although according to the projections the EU limit for BaP presence in the atmosphere of 1 ng m^{-3} will not be reached, there will be an increase in the life-time risk of lung cancer, particularly in the most populated areas.

Acknowledgements

This study was financially supported by the Spanish Ministry of Economy and Competitiveness, through the project CTM2012-33079, CGL2014-59677-R and CGL2017-87921-R (also partially funded by the FEDER European program). Noelia Domínguez Morueco received a PhD fellowship (FPI Pre-doctoral Contracts for the Formation of Doctors 2013) and a visiting research grant (EEBB-I-17-12509) from the same institution. Further support was provided under projects: (i) project CGL2014-59677-R also partially funded by FEDER; (ii) POCI-01-0145-FEDER-006939 (LEPABE -UID/EQU/00511/2013) funded by the European Regional Development Fund (ERDF), through COMPETE2020 - Programa Operacional Competitividade e Internacionalização (POCI) and by national funds, through FCT - Fundação para a Ciência e a Tecnologia; (iii) NORTE-01-0145-FEDER-000005-LEPABE-2-ECO-NNOVATION, supported by North Portugal Regional Operational Programme (NORTE 2020), under the Portugal 2020 Partnership Agreement, through the ERDF; (iv) Investigador FCT contract IF/01101/2014 (Nuno Ratola).

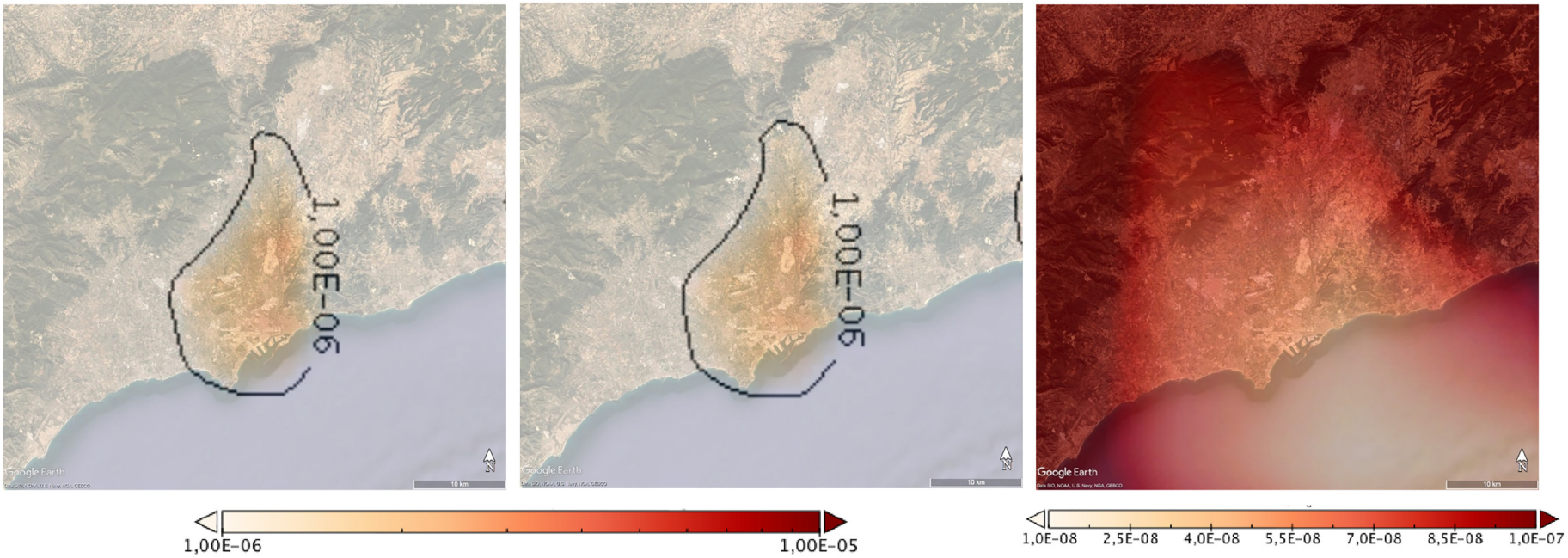

Fig. 8. – Associated increased risk of lung cancer for (left) life-time exposure to the target value (contours) for the time frame 1996–2015, and (center) for the 2031–2050 climate change projection, as defined by the Quantitative Risk Assessment included in Butterfield and Brown (2012). (Right) Differences in the increased risk of lung cancer between present and future climate change RCP8.5 scenario.

References

Andersen, A., Dahlberg, B.E., Magnus, K., Wannag, A., 1982. Risk of cancer in the Norwegian aluminium industry. Int. J. Cancer 29, 295–298.

Bernalte, E., Marín-Sánchez, C., Pinilla-Gil, E., Cerceda-Balic, F., Vidal-Cortex, V., 2012. An exploratory study of particulate PAHs in low-polluted urban and rural areas of southwest Spain: concentrations, source assignment, seasonal variation and correlations with other pollutants. Water Air Soil Pollut. 223, 5143–5154.

Bieser, J., Aulinger, A., Matthias, V., Quante, M., 2012. Impact of emission reductions between 1980 and 2020 on atmospheric benzo[a]pyrene concentrations over Europe. Water Air Soil Pollut. 223, 1393–1414.

Boylan, J.W., Russell, A.G., 2006. PM and light extinction model performance metrics, goals, and criteria for three-dimensional air quality models. Atmos. Environ. 40, 4946–4959.

Breivik, K., Vestreng, V., Rozovskaya, O., Pacyna, J.M., 2006. Atmospheric emissions of some POPs in Europe: a discussion of existing inventories and data needs. Environ. Sci. Pol. 9, 663–674.

Butterfield, D.M., Brown, R.J.C., 2012. Polycyclic aromatic hydrocarbons in Northern Ireland. National Physical Laboratory Report AS66, Teddington, Middlesex, UK.

Cabrerizo, A., Dachs, J., Barceló, D., Jones, K.C., 2012. Influence of organic matter content and human activities on the occurrence of organic pollutants in antarctic soils, lichens, grass, and mosses. Environ. Sci. Technol. 46 (3), 1396–1405.

Csiszar, S., Diamond, M.L., Thibodeaux, L.J., 2012. Modeling urban films using a dynamic multimedia fugacity model. Chemosphere 87, 1024–1031.

Csiszar, S., Daggupaty, S.M., Verkoeyen, S., Giang, A., Diamond, M.L., 2013. SO-MUM: a coupled atmospheric transport and multimedia model used to predict intraurban-scale PCB and PBDE emissions and fate. Environ. Sci. Technol. 47, 436−−445.

Dawson, J.P., Racherla, P.N., Lynn, B.H., Adams, P.J., Pandis, S.N., 2009. Impacts of climate change on regional and urban air quality in the eastern United States: role of meteorology. J. Geophys. Res. 114, D05308.

Dee, D.P., Uppala, S.M., Simmons, A.J., Berrisford, P., Poli, P., Kobayashi, S., Andrae, U., Balmaseda, M.A., Balsamo, G., Bauer, P., Bechtold, P., Beljaars, A.C.M., van de Berg, L., Bid- lot, J., Bormann, N., Delsol, C., Dragani, R., Fuentes, M., Geer, A.J., Haimberger, L., Healy, S.B., Hersbach, H., Hólm, E.V., Isaksen, L., Kållberg, P., Köhler, M., Matricardi, M., McNally, A.P., Monge-Sanz, B.M., Morcrette, J.-J., Park, B.-K., Peubey, C., de Rosnay, P., Tavolato, C., Thépaut, J.-N., Vitart, F., 2011. The ERA-interim reanalysis: configuration and performance of the data assimilation system. Q. J. R. Meteorol. Soc. 137, 553–597.

Di Guardo, A., Gouin, T., MacLeod, M., Scheringer, M., 2018. Environmental fate and exposure models: advances and challenges in 21st century chemical risk assessment. Environ. Sci.: Processes Impacts 20, 58–71.

Domínguez-Morueco, N., Diamond, M.L., Sierra, J., Schuhmacher, M., Domingo, J.L., Nadal, M., 2016. Application of the multimedia urban model to estimate the emissions and environmental fate of PAHs in Tarragona County, Catalonia, Spain. Sci. Total Environ. 573, 1622–1629.

Domínguez-Morueco, N., Augusto, S., Trabalón, L., Pocurull, E., Borrull, F., Schuhmacher, M., Domingo, J.L., Nadal, M., 2017. Monitoring PAHs in the petrochemical area of Tarragona County, Spain: comparing passive air samplers with lichen transplants. Environ. Sci. Pollut. Res. 24 (13), 11890–11900.

Domínguez-Morueco, N., Carvalho, M., Sierra, J., Schuhmacher, M., Domingo, J.L., Ratola, N., Nadal, M., 2018. Multi-component determination of atmospheric semi-volatile organic compounds in soils and vegetation from Tarragona County, Catalonia, Spain. Sci. Total Environ. 631-632, 1138–1152.

EL-Saeid, M.H., Al-Turki, A.M., Nadeem, M.E.A., Hassanin, A.S., Al-Wabel, M.I., 2015. Photolysis degradation of polyaromatic hydrocarbons (PAHs) on surface sandy soil. Environ. Sci. Pollut. Res. 22 (13), 9603–9616.

Estellano, V.H., Pozo, K., Harner, T., Corsolini, S., Focardi, S., 2012. Using PUF disk passive samplers to simultaneously measure air concentrations of persistent organic pollutants (POPs) across the Tuscany region, Italy. Atmos. Pollut. Res. 3 (1), 88–94.

Estellano, V.H., Pozo, K., Silibello, C., Mulder, M.D., Efstathiou, C., Tomasino, M.P., Furano, F., Donadio, I., Focardi, F., 2014. Characterization of urban pollution in two cities of the Puglia region in southern Italy using field measurements and air quality (AQ) model approach. Atmos. Pollut. Res. 5, 34–41.

European Commission, 2009. Directive 2004/107/EC of the European parliament and of the council of 15 December 2004 relating to arsenic, cadmium, mercury, nickel and polycyclic aromatic hydrocarbons in ambient air. Amended by regulation (EC) No 219/2009 of the European parliament and of the council of 11 March 2009. Off. J. Eur. Union 87, 1–17.

European Union, 2001. European Union Position Paper, Ambient Air Pollution by Polycyclic Aromatic Hydrocarbons (PAH). 92-894-2057-X.

Giorgetta, M., Jungclaus, J., Reick, C., Legutke, S., Brovkin, V., Crueger, T., Stevens, B., 2012a. Forcing data for regional climate models based on the MPI- ESM-LR model of the max Planck Institute for Meteorology (MPI-M): The CMIP5 historical experiment. World Data Center for Climate (WDCC) at DKRZ https://doi.org/10.1594/WDCC/RCM_CMIP5_historical-LR.

Giorgetta, M., Jungclaus, J., Reick, C., Legutke, S., Brovkin, V., Crueger, T., Stevens, B., 2012b. Forcing data for regional climate models based on the MPI- ESM-LR model of the max Planck Institute for Meteorology (MPI-M): The CMIP5 rcp85 experiment. World Data Center for Climate (WDCC) at DKRZ https://doi.org/10.1594/WDCC/RCM_CMIP5_rcp85-LR.

Guenther, A., Karl, T., Harley, P., Wiedinmyer, C., Palmer, P.I., Geron, C., 2006. Estimates of global terrestrial isoprene emissions using MEGAN (model of emissions of gases and aerosols from nature). Atmos. Chem. Phys. 6 (11), 3181–3210.

He, J., Balasubramanian, R., 2010. A comparative evaluation of passive and active samplers for measurements of gaseous semi-volatile organic compounds in the tropical atmosphere. Atmos. Environ. 44 (7), 884–891.

Huang, X., Dixon, D.G., Greenberg, B.M., 1995. Increased polycyclic aromatic hydrocarbon toxicity following their photomodification in natural sunlight: impacts on the duckweed Lemna gibba L. G-3. Ecotoxicol. Environ. Saf. 32, 194–200.

Jerez, S., Montávez, J.P., Gómez-Navarro, J.J., Lorente-Plazas, R., García-Valero, J.A., Jiménez-Guerrero, P., 2013a. A multi-physics ensemble of regional climate change projections over the Iberian Peninsula. Clim. Dyn. 41, 1749–1768.

Jerez, S., Jiménez-Guerrero, P., Montávez, J.P., Trigo, R., 2013b. Impact of the North Atlantic oscillation on European aerosol ground levels through local processes: a seasonal model-based assessment using fixed anthropogenic emissions. Atmos. Chem. Phys. 13, 11195–11207.

Jia, H., Li, L., Chen, H., Zhao, Y., Li, X., Wang, C., 2015. Exchangeable cations-mediated photodegradation of polycyclic aromatic hydrocarbons (PAHs) on smectite surface under visible light. J. Hazard. Mater. 287, 16–23.

Jiménez-Guerrero, P., Montávez, J.P., Gómez-Navarro, J.J., Jerez, S., Lorente-Plazas, R., 2012. Impacts of climate change on ground level gas-phase pollutants and aerosols in the Iberian Peninsula for the late XXI century. Atmos. Environ. 55, 483–495.

Jiménez-Guerrero, P., Gómez-Navarro, J.J., Baró, R., Lorente, R., Ratola, N., Montávez, J.P., 2013a. Is there a common pattern of future gas-phase air pollution in Europe under diverse climate change scenarios? Clim. Chang. 121, 661–671.

Jiménez-Guerrero, P., Jerez, S., Montávez, J.P., Trigo, R.M., 2013b. Uncertainties in future ozone and PM_{10} projections over Europe from a regional climate multi physics ensemble. Geophys. Res. Lett. 40, 5764–5769.

Jiménez-Guerrero, P., Montávez, J.P., Domínguez, M., Romera, R., Fita, L., Fernández, J., Cabos, W.D., Liguori, G., Gaertner, M.A., 2013c. Mean fields and interannual variability in RCM simulations over Spain: the ESCENA project. Clim. Res. 57, 201–220.

Lammel, G., Sehili, A.M., Bond, T.C., Feichter, J., Grassl, H., 2009. Gas/particle partitioning and global distribution of polycyclic aromatic hydrocarbons – a modelling approach. Chemosphere 76, 98–106.

Lang, C., Fettweis, X., Erpicum, M., 2015. Future climate and surface mass balance of Svalbard glaciers in an RCP8.5 climate scenario: a study with the regional climate model MAR forced by MIROC5. Cryosphere 9, 945–956.

Liao, K.J., Tagaris, E., Manomaiphiboon, K., Wang, C., Woo, J.H., Amar, P., He, S., Russell, A.G., 2009. Quantification of the impact of climate uncertainty on regional air quality. Atmos. Chem. Phys. 9, 865–878.

Lindstedt, G., Sollenberg, J., 1982. Polycyclic aromatic hydrocarbons in the occupational, environment, with special reference to benzo[a]pyrene measurements in Swedish industry. Scand. J. Work Environ. Health 1982 (8), 1–19.

Mackay, D., Paterson, S., 1991. Evaluating the multimedia fate of organic-chemicals - a level-III fugacity model. Environ. Sci. Technol. 25 (3), 427–436.

Mallakin, A., McConkey, B.J., Miao, G., McKibben, B., Snieckus, V., Dixon, D.G., Greenberg, B.M., 1999. Impacts of structural photomodification on the toxicity of environmental contaminants: anthracene photooxidation products. Ecotoxicol. Environ. Saf. 43 (2), 204–212.

Marquès, M., Mari, M., Audí-Miró, C., Sierra, J., Soler, A., Nadal, M., Domingo, J.L., 2016a. Photodegradation of polycyclic aromatic hydrocarbons in soils under a climate change base scenario. Chemosphere 148, 495–503.

Marquès, M., Mari, M., Audí-Miró, C., Sierra, J., Soler, A., Nadal, M., Domingo, J.L., 2016b. Climate change impact on the PAH photodegradation in soils: characterization and metabolites identification. Environ. Dermatol. Int. 89–90, 155–165.

Marquès, M., Mari, M., Sierra, J., Nadal, M., Domingo, J.L., 2017. Solar radiation as a swift pathway for PAH photodegradation: a field study. Sci. Total Environ. 581–582, 530–540.

Meinshausen, M., Smith, S.J., Calvin, K.V., Daniel, J.S., Kainuma, M.L.T., Lamarque, J.F., Matsumoto, K., Montzka, S.A., Raper, S.C.B., Riahi, K., Thomson, A.M., Velders, G.J.M., van Vuuren, D., 2011. The RCP greenhouse gas concentrations and their extension from 1765 to 2300. Clim. Chang. 109, 213–241.

Meleux, F., Solmon, F., Giorgi, F., 2007. Increase in summer European ozone amounts due to climate change. Atmos. Environ. 41, 7577–7587.

Menut, L., Bessagnet, B., Khvorostyanov, D., Beekmann, M., Blond, N., Colette, A., Coll, I., Curci, G., Foret, G., Hodzic, A., Mailler, S., Meleux, F., Monge, J.L., Pison, I., Siour, G., Turquety, S., Valari, M., Vautard, R., Vivanco, M.G., 2013. CHIMERE 2013: a model for regional atmospheric composition modelling. Geosci. Model Dev. 6, 981–1028.

Moss, R.H., Edmonds, J.A., Hibbard, K.A., Manning, M.R., Rose, S.K., Van Vuuren, D.P., Carter, T.R., Emori, S., Kainuma, M., Kram, T., Meehl, G.A., 2010. The next generation of scenarios for climate change research and assessment. Nature 463 (7282), 747–756.

Nadal, M., Mari, M., Schuhmacher, M., Domingo, J.L., 2009. Multicompartmental environmental surveillance of a petrochemical area: levels of micropollutants. Environ. Int. 35, 227–235.

Nadal, M., Marquès, M., Mari, M., Domingo, J.L., 2015. Climate change and environmental concentrations of POPs: a review. Environ. Res. 143, 177–185.

Noyes, P.D., McElwee, M.K., Miller, H.D., Clark, B.W., Van Tiem, L.A., Walcott, K.C., Erwin, K.N., Lavin, E.D., 2009. The toxicology of climate change: environmental contaminants in a warming world. Environ. Int. 35 (6), 971–986.

Odabasi, M., Dumanoglu, Y., Kara, M., Altiok, H., Elbir, T., Bayram, A., 2017. Spatial variation of PAHs and PCBs in coastal air, seawater, and sediments in a heavily industrialized region. Environ. Sci. Pollut. Res. 24, 13749–13759.

Pistocchi, A., Sarigiannis, D.A., Vizcaino, P., 2010. Spatially explicit multimedia fate models for pollutants in Europe: state of the art and perspectives. Sci. Total Environ. 408, 3817–3830.

Pöschl, U., Letzel, T., Schauer, C., Niessner, R., 2001. Interaction of ozone and water vapor with spark discharge soot aerosol particles coated with benzo[a]pyrene: O_3 and H_2O adsportion, benzo[a]pyrene degradation, and atmospheric implications. J. Phys. Chem. A 105, 4029–4041.

Ras, M.R., Marcé, R.M., Cuadras, A., Mari, M., Nadal, M., Borrull, F., 2009. Atmospheric levels of polycyclic aromatic hydrocarbons in gas and particulate phases from Tarragona region (NE Spain). Int. J. Environ. Anal. Chem. 89, 543–556.

Ratola, N., Jiménez-Guerrero, P., 2015. Combined field/modelling approaches to represent the air-vegetation distribution of benzo[a]pyrene using different vegetation species. Atmos. Environ. 106, 34–42.
Ratola, N., Jiménez-Guerrero, P., 2016. Can biomonitors effectively detect airborne benzo [a]pyrene? An evaluation approach using modelling. Atmospheric. Chem. Phys. 16 (7), 4271–4282.
Ratola, N., Jiménez-Guerrero, P., 2017. Modelling benzo[a]pyrene in air and vegetation for different land uses and assessment of increased health risk in the Iberian Peninsula. Environ. Sci. Pollut. Res. 24 (13), 11901–11910.
RIVM, 1989. Integrated Criteria Document PAH. National Institute of Public Health and Environmental Protection, Bilthoven.
San José, R., Pérez, J.L., Callén, M.S., López, J.M., Mastral, A., 2013. BaP (PAH) air quality modelling exercise over Zaragoza (Spain) using an adapted version of WRF-CMAQ model. Environ. Pollut. 183, 151–158.
Schneider, P., Castell, N., Vogt, M., Dauge, F.R., Lahoz, W.A., Bartonova, A., 2017. Mapping urban air quality in near real-time using observations from low-cost sensor and model information. Environ. Int. 106, 234–247.
Schwarzenbach, R.P., Gschwend, P.M., Imboden, D.M., 2003. Environmental Organic Chemistry. 2nd Ed. John Wiley & Sons, Hoboken, New Jersey.
Silva, J.A., Ratola, N., Ramos, S., Homem, V., Santos, L., Alves, A., 2015. An analytical multi-residue approach for the determination of semi-volatile organic pollutants in pine needles. Anal. Chim. Acta 858, 24–31.
Skamarock, W.C., Klemp, J.B., Dudhia, J., Gill, D.O., Barker, D.M., Duda, M.G., 2008. A Description of the Advanced Research WRF Version 3. NCAR Technical Note NCAR/TN20201c475+STR. 2008 Available at. http://www2.mmm.ucar.edu/wrf/users/docs/arw_v3.pdf.
Srogi, K., 2007. Monitoring of environmental exposure to polycyclic aromatic hydrocarbons: a review. Environ. Chem. Lett. 5 (4), 169–195.
Sulas, L., Franca, A., Sanna, F., Re, G.A., Melis, R., Porqueddu, C., 2015. Biomass characteristics in Mediterranean populations of *Piptatherum miliaceum*-a native perennial grass species for bioenergy. Ind. Crop. Prod. 75, 76–84.
Taylor, K.E., Stouffer, R.J., Meehl, G.A., 2012. An overview of CMIP5 and the experiment design. Bull. Am. Meteorol. Soc. 93 (4), 485–498.
Vestreng, V., Ntziachristos, L., Semb, A., Reis, S., Isaksen, I.S.A., Tarrasón, L., 2009. Evolution of NOx emissions in Europe with focus on road transport control measures. Atmos. Chem. Phys. 9, 1503–1520.
World Health Organisation, 2000. Air Quality Guidelines. Chapter 5.9 - PAHs. 2nd edition. September 2000.
Yu, M., Wang, G., Parr, D., Ahmed, K.F., 2014. Future changes of the terrestrial ecosystem based on a dynamic vegetation model driven with RCP8.5 climate projections from 19 GCMs. Clim. Chang. 127 (2), 257–271.
Zabiegała, B., Kot-Wasik, A., Urbanowicz, M., Namieśnik, J., 2010. Passive sampling as a tool for obtaining reliable analytical information in environmental quality monitoring. Anal. Bioanal. Chem. 396 (1), 273–296.
Zhang, L., L I, P., Gong, Z., Oni, A., 2006. Photochemical behavior of benzo [a] pyrene on soil surfaces under UV light irradiation. J. Environ. Sci. 18 (6), 1226–1232.